Molecular Pharmacology Fast Forward. Published on May 6, 2021 as DOI: 10.1124/molpharm.120.000076
This article has not been copyedited and formatted. The final version may differ from this version.

Title Page:

Differential In vitro Pharmacological Profiles of Structurally Diverse Nociceptin Receptor Agonists in Activating G-protein and Beta-arrestin Signaling at the Human Nociceptin Opioid Receptor

James J. Lu, Willma E. Polgar, Anika Mann, Pooja Dasgupta, Stefan Schulz, and Nurulain T. Zaveri*

J.J.L., W.E.P. and N.T.Z., Astraea Therapeutics, 320 Logue Avenue, Suite 142, Mountain View, CA 94043, USA

A.M., P.D. and S.S., Institute of Pharmacology and Toxicology, Jena University Hospital, Friedrich Schiller University Jena, Drackendorfer Str. 1, 07747, Jena, Germany

Molecular Pharmacology Fast Forward. Published on May 6, 2021 as DOI: 10.1124/molpharm.120.000076
This article has not been copyedited and formatted. The final version may differ from this version.

Running Title Page:

Running Title: Differential Signaling Profiles of Diverse NOP Agonists

***Address correspondence to:**

Dr. Nurulain T. Zaveri

Astraea Therapeutics, LLC.

320 Logue Avenue, Suite 142,

Mountain View, CA 94043, USA.

Tel: 650-254-0786

Email: nurulain@astraeatherapeutics.com

Number of text pages: 45

Number of tables: 3

Number of figures: 5

Number of references: 62

Number of words in the abstract: 250

Number of words in the Introduction: 750 (not including citations)

Number of words in the Discussion: 1401 (not including citations)

List of abbreviations:

cAMP, 3',5'-cyclic adenosine monophosphate; CHO, Chinese hamster ovary; CPM, counts per minute; DMEM, Dulbecco's modified Eagle's medium; FBS, fetal bovine serum; GIRK, G protein-dependent inwardly rectifying potassium channel; MOR, mu opioid peptide receptor; N/OFQ, nociceptin/orphanin FQ; NOP, nociceptin opioid peptide receptor; ORL, opioid receptor-like receptor

Molecular Pharmacology Fast Forward. Published on May 6, 2021 as DOI: 10.1124/molpharm.120.000076
This article has not been copyedited and formatted. The final version may differ from this version.

ABSTRACT

Agonists at the nociceptin opioid peptide receptor (NOP) are under investigation as therapeutics for non-addicting analgesia, opioid use disorder, Parkinson's disease, and other indications. NOP full and partial agonists have both been of interest, particularly since NOP partial agonists show a reduced propensity for behavioral disruption than NOP full agonists. Here, we investigated the in vitro pharmacological properties of chemically diverse NOP receptor agonists in assays measuring functional activation of the NOP receptor such as GTPγS binding, cAMP inhibition, GIRK activation, phosphorylation, β-arrestin recruitment and receptor internalization. When normalized to the efficacy of the natural agonist nociceptin/orphanin FQ (N/OFQ), we found that different functional assays that measure intrinsic activity produce inconsistent levels of agonist efficacy, particularly for ligands that were partial agonists. Agonist efficacy obtained in the GTPγS assay tended to be lower than that in the cAMP and GIRK assays. These structurally diverse NOP agonists also showed differential receptor phosphorylation profiles at the phosphosites we examined and induced varying levels of receptor internalization. Interestingly, while the rank order for β-arrestin recruitment by these NOP agonists was consistent with their ability to induce receptor internalization, their phosphorylation signatures at the timepoint we investigated were not indicative of the levels of β-arrestin recruitment or internalization induced by these agonists. It is possible that other phosphorylation sites, yet to be identified, drive the recruitment of NOP receptor ensembles and subsequent receptor trafficking by some nonpeptide NOP agonists. These findings potentially help understand NOP agonist pharmacology in the context of ligand-activated receptor trafficking.

Molecular Pharmacology Fast Forward. Published on May 6, 2021 as DOI: 10.1124/molpharm.120.000076
This article has not been copyedited and formatted. The final version may differ from this version.

Significance Statement:

Chemically diverse agonist ligands at the nociceptin opioid receptor GPCR showed differential efficacy for activating downstream events after receptor binding, in a suite of functional assays measuring GTPγS binding, cAMP inhibition, GIRK channel activation, β-arrestin recruitment, receptor internalization and receptor phosphorylation. These analyses provide a context for understanding NOP agonist pharmacology driven by ligand-induced differential NOP receptor signaling.

Molecular Pharmacology Fast Forward. Published on May 6, 2021 as DOI: 10.1124/molpharm.120.000076
This article has not been copyedited and formatted. The final version may differ from this version.

INTRODUCTION

The nociceptin/orphanin FQ receptor opioid (NOP) receptor is the last discovered member of the opioid G protein-coupled receptor (GPCR) family (Bunzow et al., 1994; Fukuda et al., 1994; Lachowicz et al., 1995; Mollereau et al., 1994), and is a G_i/G_o coupled receptor like the classical opioid receptors mu, delta and kappa (MOR, KOP and DOP respectively). The endogenous ligand for the NOP receptor is a heptadecapeptide, nociceptin/orphaninFQ (N/OFQ), which only binds the NOP receptor and has no affinity for the classical opioid receptors (Meunier et al., 1995; Reinscheid et al., 1995). As with classical opioid receptors, activation of NOP by N/OFQ or synthetic agonists leads to inhibition of adenylate cyclase and 3',5'-cyclic adenosine monophosphate (cAMP) production, inhibition of calcium channels and activation of G protein-coupled inwardly rectifying potassium channels (GIRK) (Hawes et al., 2000; Ikeda et al., 1997; Mollereau et al., 1994). While not completely understood, key signal transduction pathways activated after ligand binding to the NOP GPCR have been investigated (Toll et al., 2016). Ligand binding to the cell surface NOP receptor leads to binding of the inhibitory heterotrimeric $G_{i/o}$ G protein, followed by dissociation of the Gα subunit, resulting in the inhibition of adenylate cyclase activity and decrease in the intracellular levels of cAMP. The Gβγ subunits couple to and activate GIRK channels, increasing potassium current (Connor et al., 1996a; Vaughan and Christie, 1996) and suppressing voltage-dependent calcium channels (Beedle et al., 2004; Connor et al., 1996b), resulting in cell hyperpolarization. This channel modulation upon agonist binding to the NOP receptor is consistent with the inhibitory actions of N/OFQ and agonists on neuronal activity and neurotransmitter release.

Like other GPCRs, NOP signaling and function are regulated by phosphorylation, internalization and receptor desensitization (See (Donica et al., 2013) for an excellent review). The Gβγ subunits that dissociate from the G protein-receptor complex recruit G protein receptor kinases

Molecular Pharmacology Fast Forward. Published on May 6, 2021 as DOI: 10.1124/molpharm.120.000076
This article has not been copyedited and formatted. The final version may differ from this version.

(GRKs) for phosphorylation of GPCR intracellular domains. The agonist-bound phosphorylated GPCR undergoes a conformational change, allowing arrestin recruitment, receptor internalization and desensitization, as shown for the MOR receptor (Williams et al., 2013). The NOP receptor contains several serine, threonine and tyrosine residues within its intracellular loops and C-terminal domain that can act as substrates for GRK-mediated NOP receptor phosphorylation. Using phosphosite specific antibodies, Mann et al. recently showed that NOP C-terminal residues Ser346, Ser351, and Thr362/Ser363 were phosphorylated after treatment with diverse NOP agonists in a spatial and temporal manner, with Ser346 being the first site of phosphorylation (Mann et al., 2019). GRK2 and GRK3 were shown to be important for agonist-induced phosphorylation and receptor desensitization (Mandyam et al., 2002; Mandyam et al., 2003; Mann et al., 2019; Thakker and Standifer, 2002). Further, alanine mutation of Ser363, which is phosphorylated by GRK3, reduced β-arrestin2 recruitment and NOP internalization (Zhang et al., 2012).

Arrestin recruitment by nonpeptide NOP ligands has been investigated in a limited number of studies, some of which included NOP full agonist AT-403 and NOP partial agonist AT-090 and AT-004 characterized here (Chang et al., 2015; Ferrari et al., 2016; Ferrari et al., 2017; Malfacini et al., 2015). NOP full agonist AT-403 showed significant arrestin recruitment but also activated G protein-mediated recruitment to the same extent, similar to the endogenous agonist N/OFQ (Ferrari et al., 2017). On the other hand, NOP partial agonist AT-090 (21% agonist efficacy in the GTPγS binding assay, (Ferrari et al., 2016)) showed significant efficacy for arrestin recruitment (Ferrari et al., 2016), unlike NOP partial agonist AT-004, which also showed ~20% agonist efficacy in GTPγS binding, but was nearly inactive in recruiting β-arrestin (Chang et al., 2015; Ferrari et al., 2016; Malfacini et al., 2015). These NOP ligands have not been previously

Molecular Pharmacology Fast Forward. Published on May 6, 2021 as DOI: 10.1124/molpharm.120.000076
This article has not been copyedited and formatted. The final version may differ from this version.

characterized for their effects on NOP receptor phosphorylation or internalization, but their differential efficacy of arrestin recruitment suggests that chemically diverse NOP agonists can have differential effects on NOP receptor signaling and trafficking. Here, we profiled phosphorylation signatures, arrestin recruitment and receptor internalization induced by diverse NOP agonists. We also characterized the intrinsic activity of these ligands in mediating G protein-mediated downstream events. Commonly used assays to measure functional efficacy of opioid ligands in G protein-mediated signaling include simple proximal measurements of G protein recruitment like the GTPγS binding assay (McDonald and Lambert, 2010; Sim et al., 1996) as well as other assays of downstream G protein-mediated signaling such as cAMP inhibition (Hill et al., 2010; Knapman et al., 2014), calcium release (Camarda et al., 2009; Coward et al., 1999), and GIRK activation (Parsons and Hirasawa, 2011). These assays often provide inconsistent measures of intrinsic activity for the same ligand, and such inconsistencies become particularly significant when agonist efficacy obtained in non-amplified assay systems such as GTPγS assays are compared with that obtained in amplified assay systems such as the cAMP and GIRK assays. Levels of agonist efficacy seen in different G-protein assays can also be confounded by receptor reserve, as agonists can produce a maximum response by occupying only a fraction of receptors (Selley et al., 1998; Traynor and Nahorski, 1995; Gillis et al., 2020; Kelly, 2013). Receptor reserve can also account for signal amplification and confound experimental measures of agonist efficacy, particularly when characterizing partial agonists in heterologous transfected cells (Adham et al., 1993; Baker et al., 2000; Selley et al., 1998; Traynor and Nahorski, 1995).

Here, we investigated the functional efficacy of several selective NOP agonists from our NOP ligand library, using multiple G-protein assays and determined the range of intrinsic activity

Molecular Pharmacology Fast Forward. Published on May 6, 2021 as DOI: 10.1124/molpharm.120.000076
This article has not been copyedited and formatted. The final version may differ from this version.

obtained amongst various assays for the same ligand. We also investigated the phosphorylation profiles, arrestin recruitment and receptor internalization induced by these selective NOP agonists and found differential ligand-induced NOP receptor signaling and trafficking among the NOP ligands we examined.

Molecular Pharmacology Fast Forward. Published on May 6, 2021 as DOI: 10.1124/molpharm.120.000076
This article has not been copyedited and formatted. The final version may differ from this version.

MATERIALS AND METHODS

Chemical compounds. NOP-selective ligands AT-004 (Kamakolanu et al., 2020), AT-090 (Ferrari et al., 2016), AT-200 (Zaveri et al., 2004), AT-312 (Zaveri et al., 2018b), AT-390 (Arcuri et al., 2018) and AT-403 (Arcuri et al., 2018) were synthesized at Astraea Therapeutics and have been previously reported. Stock solutions of N/OFQ at a 1 mM concentration and DAMGO at a 10 mM concentration were prepared in deionized water, whereas those of the AT-ligands were prepared in DMSO (10 mM) and diluted with water or assay medium to the desired concentration.

Cell culture and transfection. All cells were maintained in a 5% CO_2 incubator under saturated humidity and 37 ^{o}C. Human NOP (hORL) and MOR (hMOR) opioid receptors were stably expressed individually in Chinese hamster ovary (CHO) cells as reported previously (Zaveri et al., 2001). The hORL CHO cells were cultured in 150 mm tissue culture dishes (Corning, New York City, NY) in Dulbecco's Modified Eagle's Medium (DMEM, Gibco, Thermo Fisher Scientific, Waltham, MA) supplemented with 10% fetal bovine serum (FBS), 100 U/ml penicillin, 100 μg/ml streptomycin and 400 μg/ml G418. The hMOR CHO cells were cultured in 50% F12/DMEM (Gibco, Thermo Fisher Scientific, Waltham, MA) supplemented with 10% FBS, 100 U/ml penicillin, 100 μg/ml streptomycin and 400 μg/ml G418. The AtT-20/D16v-F2 (AtT-20) cells used in GIRK assays were purchased from the American Type Culture Collection and cultured in DMEM supplemented with 10% FBS, 2 mM L-glutamine, 100 U/ml penicillin, and 100 μg/ml streptomycin. The HTLA cells (a HEK293 cell line stably expressing a tTA-dependent luciferase reporter and a β-arrestin2-TEV fusion gene) used for β-arrestin assays were a gift from Dr. Bryan Roth and cultured in DMEM supplemented with 10% FBS, 100 U/ml penicillin, 100 μg/ml streptomycin, 100 μg/ml hygromycin B and 2 μg/ml puromycin. Then, the HTLA cells were transiently transfected with NOP or MOR receptors overnight before the β-

Molecular Pharmacology Fast Forward. Published on May 6, 2021 as DOI: 10.1124/molpharm.120.000076
This article has not been copyedited and formatted. The final version may differ from this version.

arrestin assays were carried out (see details below). For cAMP assays, the hORL and hMOR CHO cells were transiently transfected with a cAMP23F plasmid (Promega, Madison, WI) overnight before the cAMP assays were carried out (see details below).

Membrane preparation. The hORL and hMOR CHO cells were grown to confluency and harvested for membrane preparation. The membrane was prepared in 50 mM Tris buffer (pH 7.4). Cells were scraped off 150 mm culture dishes and centrifuged at 500 × g for 15 min. The cell pellet was homogenized in 50 mM Tris with a Fisher Scientific PowerGen 125 rotor-stator type homogenizer, centrifuged at 20,000 × g for 25 min, washed and re-centrifuged once more at 20,000 × g for 25 min, aliquoted at a concentration of 2 mg/ml protein per vial for hORL and 3 mg/ml protein per vial for hMOR, and stored in a –80 °C freezer until use.

Receptor binding assay. AT compounds were dissolved in 100% DMSO to a concentration of 10 mM. The binding assays were performed in 96-well polystyrene plates using six concentrations of each test compound (final concentration of 10 μM to 0.1 nM in 10-fold dilutions) in triplicate, with each well containing 100 μl of compound and 100 μl of tritiated ligands [^{3}H]DAMGO (48.0 Ci/mmol, K_d 0.69 nM for MOR) or [^{3}H]N/OFQ (130 Ci/mmol, K_d 0.065 nM for NOP). Nonspecific binding was determined using 1.0 μM of the unlabeled nociceptin for NOP and 1.0 μM of unlabeled DAMGO for MOR. Assays were initiated by the addition of 800 μl of membrane per well, after which the samples were incubated for 60 min at 25 °C in a total volume of 1.0 ml. In NOP receptor experiments, 1 mg/ml BSA was added to the compound dilution buffer. The incubation was terminated by rapid filtration through 0.05% PEI-soaked glass fiber filter mats (GF/C Filtermat A, Perkin Elmer) on a Tomtec Mach III cell harvester and washed 5 times with 0.5 ml of ice-cold 50 nM Tris-HCl (pH 7.4) buffer. The filters were dried overnight and soaked with scintillation cocktail before counting on a Wallac Beta

Molecular Pharmacology Fast Forward. Published on May 6, 2021 as DOI: 10.1124/molpharm.120.000076
This article has not been copyedited and formatted. The final version may differ from this version.

plate 1205 liquid scintillation counter. Radioactivity was determined as counts per minute (CPM). IC_{50} values were determined using at least six concentrations of test compound and calculated using the variable slope curve-fitting method in GraphPad Prism 6.0 software (ISI, San Diego, CA). K_i values were determined by the method of Cheng and Prusoff (Cheng and Prusoff, 1973).

[^{35}S] GTPγS binding assay. [^{35}S] GTPγS binding assays were conducted as previously described (Khroyan et al., 2011; Toll et al., 2009). In brief, membranes (2 mg/ml protein for NOP and 3 mg/ml for MOR) were incubated for 60 min at 25 °C with [^{35}S] GTPγS (50 pM), GDP (10 μM), and the appropriate compound, in a total volume of 1.0 ml Buffer A containing 20 mM HEPES, 10 mM $MgCl_2$, and 100 mM NaCl (pH 7.4). Samples were filtered over glass fiber filters and counted as described for the binding assays. Agonist efficacy (Emax) is reported as % maximal stimulation relative to the standard full agonist N/OFQ or DAMGO and calculated as (maximal stimulation by test compound ÷ maximal stimulation by standard full agonist ×100),. The EC_{50} values were calculated using the variable slope dose-response curve fitting method in GraphPad Prism 6.0 software.

GloSensor cAMP assay. The plasmid pGloSensor-23F-cAMP was transfected into hORL and hMOR CHO cells (1.5×10^6 cells) using the Fugene 6 HD reagent (Promega, Madison, WI). 24 h after the transfection, the cells were harvested, suspended in the culture medium, and seeded (100 μl/well at a concentration of 1×10^5 cells/ml) into 96-well white wall microtiter plates. After being incubated at 37 °C for 24 h in a humidified environment containing 5% CO_2, the medium was replaced with DMEM containing 6% GloSensor cAMP substrate (Promega, Madison, WI). After 2 h of additional incubation at room temperature, different AT compounds at 5 concentrations (final concentration of 1 μM to 0.1 nM in 10-fold dilutions) were added into the wells for 15 min of incubation, followed by the addition of 10 μM of forskolin (final

Molecular Pharmacology Fast Forward. Published on May 6, 2021 as DOI: 10.1124/molpharm.120.000076
This article has not been copyedited and formatted. The final version may differ from this version.

concentration) to stimulate cAMP synthesis. Then, the dynamic luminescence signal of the wells was detected immediately using a FluoStar Optima plate reader (BMG, Gütersloh, Germany) for 30 consecutive minutes at a rate of 1 read/well/sec. Subsequently, to calculate Emax of the standard agonist, cAMP inhibition induced by 1 μM of the positive control N/OFQ or DAMGO in the presence of 10 μM of forskolin (i.e., the max level of cAMP signal in the presence of 1 μM N/OFQ or DAMGO plus 10 μM forskolin divided by the max level of cAMP signal in the presence of 10 μM forskolin only) was used as 100%, and the level of cAMP inhibition induced by test compounds was normalized to that of N/OFQ or DAMGO (net cAMP inhibition by test compound ÷ net cAMP inhibition by 1 μM full agonist × 100). In addition, the IC_{50} of different compounds in inhibiting cAMP synthesis was calculated using the variable slope dose-response curve fitting method in GraphPad Prism 6.0 software. In order to minimize intra-assay variations caused by transient transfections carried out on different days, the key time points of the assay, including the time of transfection, the time of compound, forskolin and reagent addition, and the time of signal readout on the plate reader, were kept the same among different days. Furthermore, only the experiments showing comparable baseline (negative control) and positive control (N/OFQ or DAMGO) signals were included in the comparative analyses to ensure intra-assay consistency.

GIRK assay. AtT-20 cells stably expressing hNOP or hMOR receptors were plated in 96-well black, clear bottom plates covered with poly-L-lysine. Plates were kept for 48 h at 37 °C and 5% CO_2. Assay was performed as previously described (Günther et al., 2016) using Hank's balanced salt solution (HBSS), buffered with HEPES 20 mM (pH 7.4) as standard buffer. The membrane potential dye FMP (FLIPR Membrane Potential kit BLUE, Molecular Devices, Biberach, Germany) was reconstituted according to manufacturer's instructions. Test compounds were

Molecular Pharmacology Fast Forward. Published on May 6, 2021 as DOI: 10.1124/molpharm.120.000076
This article has not been copyedited and formatted. The final version may differ from this version.

prepared right before assay measurements at the concentration indicated. The assay was performed in a FlexStation 3 microplate reader (Molecular Devices, Biberach, Germany).

Western Blot Analysis (Receptor Phosphorylation). Stably transfected HEK293 cells expressing human NOP receptors were plated onto poly-L-lysine-coated 60-mm dishes and grown for 2 days to 80% confluency. After incubating with 10 μM N/OFQ or agonists for 10 min at 37 °C, the cells were lysed with a detergent buffer (50 mM Tris-HCl, pH 7.4; 150 mM NaCl; 5 mM EDTA; 10 mM NaF; 10 mM disodium pyrophosphate; 1% Nonidet P-40; 0.5% sodium deoxycholate; 0.1% SDS) in the presence of protease and phosphatase inhibitors. After 30 min of centrifugation at 4 °C, HA-tagged NOP receptors were enriched using anti-HA-agarose beads. Samples were then inverted for 1.5 h at 4 °C. After washing, proteins were eluted using an SDS sample buffer for 30 min at 50 °C, and proteins were separated on 7.5% or 12% SDS-polyacrylamide gels. After electroblotting, membranes were incubated with either 0.1 g/ml anti-human-pS346 (5034), anti-human-pS351 (4876) or anti-human-pT362/S363 (4874) antibodies overnight at 4 °C, followed by detection of bound antibodies using an enhanced chemiluminescence buffer (ECL) (Thermo Fisher Scientific, Schwerte, Germany). Blots were subsequently stripped and reprobed with the phosphorylation-independent anti-NOPR antibody (4871) or anti-HA antibody (0631) to ensure equal loading of the gels.

Analysis of NOP receptor internalization. Stably transfected cells expressing HA-tagged human NOP receptors were plated onto poly-L-lysine-coated coverslips and grown overnight. Cells were incubated with rabbit anti-HA antibody (0631) in serum-free medium for 2 h at 4 °C. After 60 min of agonist exposure at room temperature, cells were fixed with 4% paraformaldehyde and 0.2% picric acid in a phosphate buffer (pH 6.9) for 30 min at room temperature. Subsequently, cells were washed several times with a phosphate buffer (22.6 ml/L

Molecular Pharmacology Fast Forward. Published on May 6, 2021 as DOI: 10.1124/molpharm.120.000076
This article has not been copyedited and formatted. The final version may differ from this version.

1M $NaH_2PO_4 \cdot H_2O$; 77.4 ml/L 1M $Na_2HPO_4 \cdot H_2O$; 0.1 % Triton X-100, pH 7.4), permeabilized and then incubated with an Alexa488-coupled goat anti-rabbit antibody (Invitrogen, Darmstadt, Germany). Cells were mounted and the internalization of receptors was examined using a Zeiss LSM510 META laser scanning confocal microscope (Jena, Germany).

For quantitative internalization assays, cells were plated onto 24-well plates and grown overnight. Then, the cells were pre-incubated with anti-HA antibody (0631) for 2 h at 4 °C and exposed to agonists for 60 min at 37 °C. Subsequently, cells were fixed for 45 min at room temperature, washed 3 times with PBS and incubated with a peroxidase-conjugated secondary antibody (Santa Cruz, Heidelberg, Germany). After washing, ABTS substrate [2,2'-azino-bis(3-ethylbenzothiazoline-6-sulfonic acid) diammonium salt] was added and optical density was measured at 405 nm using a FlexStation 3 microplate reader (Molecular Devices, Biberach, Germany).

β-arrestin recruitment assay. The β-arrestin recruitment assay was carried out based on the method described previously (Allen et al., 2011). In brief, on the night prior to transfection (Day 1), HTLA cells were plated at 10×10^6 cells in 150 mm cell culture dishes (Corning, New York City, NY). On the following day when cells grew to 80% confluency (Day 2), the cells were transfected with human NOP or MOP receptors using the Fugene 6 HD transfection reagent (Promega, Madison, WI) following the protocol provided by the manufacturer. The ratio of DNA plasmid to Fugene 6 HD transfection reagent in the transfection was 1 μg DNA:6 μl Fugene 6 HD. 30 μg DNA were used for the transfection of cells in each culture dish. After 24 h of transfection (Day 3), transfected cells were harvested by trypsinization (Trypsin-EDTA, Gibco, Thermo Fisher Scientific, Waltham, MA) and then seeded into white flat-bottom 96-well tissue culture plates (Corning, New York City, NY) at 5×10^4 cells per well. 24 h later (Day 4), the

Molecular Pharmacology Fast Forward. Published on May 6, 2021 as DOI: 10.1124/molpharm.120.000076
This article has not been copyedited and formatted. The final version may differ from this version.

cells were treated with corresponding AT compounds or positive controls (DAMGO or N/OFQ for MOR and NOP, respectively) for 18 h at 37 ^{o}C. On Day 5, the luciferase signal in each well was detected by using a Bright Glo Luciferase Reporter Assay (Promega, Madison, WI) on a plate reader (BMG, FluoStar Optima, Gütersloh, Germany). The level of β-arrestin recruitment was determined by subtracting the baseline signal (medium only) from the signal detected in the presence of compound. Furthermore, to calculate % β-arrestin recruitment, the amount of β-arrestin recruitment induced by the positive control N/OFQ/DAMGO (1 μM) was used as 100%, and the amount of β-arrestin recruitment induced by AT compounds was normalized to that of N/OFQ or DAMGO. In addition, the EC_{50} values were calculated using the variable slope dose-response curve fitting method in GraphPad Prism 6.0 software. Each experiment was repeated at least 3 times, with each drug concentration in quintuplicate wells to obtain and report the average value ± standard deviation. Similar to our approach in the cAMP inhibition assay, we carried out the operations of the β-arrestin recruitment assay at fixed time points to minimize intra-assay variations. We also only included the experiments showing comparable baseline (negative control) and positive control (N/OFQ or DAMGO) signals for comparison.

Data analysis. Experimental data in Tables 1-3 were expressed as mean ± standard deviation. IC_{50} and EC_{50} values were calculated with GraphPad Prism 6.0 (GraphPad software, La Jolla, CA) using the respective curve-fitting methods indicated in the above Methods. Standard deviation was derived using the standard deviation function (stdev) in EXCEL software. For Western blot assays, the detected protein bands were quantified using ImageJ 1.47v software (National Institute of Health, Bethesda, MD). Statistical analysis for Figure 3C was carried out with Student's t-test. A p value of < 0.05 was considered statistically significant. Since this was

Molecular Pharmacology Fast Forward. Published on May 6, 2021 as DOI: 10.1124/molpharm.120.000076
This article has not been copyedited and formatted. The final version may differ from this version.

an exploratory study, a graphical representation was used to compare ligand efficacies between β-arrestin recruitment and internalization, as shown in Figure 5.

Molecular Pharmacology Fast Forward. Published on May 6, 2021 as DOI: 10.1124/molpharm.120.000076
This article has not been copyedited and formatted. The final version may differ from this version.

RESULTS

Binding affinity of AT compounds for NOP and MOR receptors. All tested NOP agonists (Figure 1) showed high binding affinity with K_i values ranging from 0.3 to 9.8 nM at the recombinant NOP receptor and from 6.0 to 375.5 nM at the recombinant MOR receptor expressed in CHO cells (Table 1). Ligands were grouped into highly selective NOP ligands with NOP selectivity > 35-fold over the MOR receptor (AT-403, AT-390, and AT-004), and modestly selective NOP ligands with NOP selectivity ranging from 17 to 26-fold (AT-200, AT-312 and AT-090) over the MOR receptor.

Intrinsic activity in the GTPγS binding assay at NOP and MOR receptors. Agonist potency and efficacy were measured in the GTPγS binding assay using membranes from CHO cells expressing human NOP or MOR receptors. Percentage of stimulation was determined by normalization to maximum activity elicited by standard full agonists N/OFQ and DAMGO. At NOP, AT-312, AT-390, and AT-403 displayed full agonist efficacy (~100% of the standard N/OFQ), whereas AT-200 > AT-004 > AT-090 showed less than 50% efficacy compared to N/OFQ (Table 2, see also Figures S1 in Supplemental Information). Based on this, the compounds were grouped into NOP full agonists (AT-312, AT-390, and AT-403) and NOP partial agonists (AT-004, AT-200, and AT-090) (Table 2). With respect to potency, the EC_{50} values of all compounds at NOP were consistently greater than their Ki values (Adapa and Toll, 1997). At MOR, all compounds showed significantly lower potency as well as lower efficacy compared to standard agonist DAMGO, consistent with their lower binding affinity at MOR.

cAMP assay at NOP and MOR receptors. In hORL or hMOR CHO cells transiently expressing the cAMP plasmid, both N/OFQ and DAMGO decreased forskolin-induced cAMP accumulation, yielding potencies (EC_{50}) of 2.2 nM for N/OFQ and 9.1 nM for DAMGO,

Molecular Pharmacology Fast Forward. Published on May 6, 2021 as DOI: 10.1124/molpharm.120.000076
This article has not been copyedited and formatted. The final version may differ from this version.

respectively (Table 2) (See also graphs of cAMP experiments in Supplemental data Figure S2). All AT compounds displayed high efficacy (85-106%) relative to N/OFQ at the NOP receptor, in rank order AT-403 > AT-090 > AT-390 > AT-312 > AT-200 > AT-004 (Table 2). Notably, the potencies for all the compounds in the NOP cAMP assay were consistently higher compared to those obtained in the GTPγS binding assay (Table 2). Further, while the NOP full agonists in the GTPγS assay (AT-312, AT-390 and AT-403) also showed full agonist efficacy in the cAMP assay, the AT compounds that showed partial agonist efficacy at NOP in the GTPγS assay (AT-004, AT-090 and AT-200) all showed nearly full agonist efficacy, but lower potencies than N/OFQ (Table 2), with exception of AT-090, which showed significantly increased potency and full agonist efficacy in the cAMP assay compared to the GTPγS binding assay.

At the MOR receptor, efficacy of the compounds obtained in the cAMP assay was also higher than that obtained via the GTPγS binding assay (Table 2), although the differences were less pronounced since these compounds had lower potency and efficacy at the MOR overall.

GIRK channel activation by AT compounds at NOP and MOR receptors. In the GIRK assay in AtT-20 cells expressing NOP or MOR receptor, both N/OFQ and DAMGO induced agonist-dependent membrane hyperpolarization in a concentration-dependent manner, yielding EC_{50} values of 1.2 nM for N/OFQ and 1.0 nM for DAMGO (Table 2), respectively, consistent with potencies we previously reported for these agonists (Mann et al., 2019). The AT compounds tested in this assay all displayed full agonist efficacy (95-105%) at NOP receptor compared to N/OFQ, in rank order AT-312 > AT-200 > AT-004 (see also graphs in Figure S3, Supplemental Information). Moreover, similar to the observations in the cAMP assay, the EC_{50} (potency) values from the GIRK assay at the NOP receptor were consistently shifted to lower values (higher potency) compared to those obtained in the GTPγS binding assay (i.e. the compounds

Molecular Pharmacology Fast Forward. Published on May 6, 2021 as DOI: 10.1124/molpharm.120.000076
This article has not been copyedited and formatted. The final version may differ from this version.

appeared more potent in the GIRK assay than in the GTPγS functional assay). Further, the efficacies of the compounds obtained from the GIRK assay were also higher than those obtained in the GTPγS binding assay. For example, AT-004 appears to be a low-efficacy partial agonist at NOP in the GTPγS assay, but showed nearly full agonist efficacy and higher potency in the NOP GIRK assay.

The differences in the levels of intrinsic activity at NOP obtained from the GTPγS binding assay, GIRK assay and cAMP assay for selected NOP ligands (AT-004, AT-200 and AT-312) are shown in Figure 2. It can be seen that the intrinsic activity observed in the GIRK and cAMP assays are significantly higher than the stimulation achieved by these compounds in the GTPγS binding assay, especially for compounds behaving as partial agonists in the GTPγS assay, i.e., a stimulation level of 20%-60% (AT-004 and AT-200). AT-090 (Table 2) also showed partial agonist efficacy in the GTPγS assay (21% stimulation) but showed full agonist efficacy (104% stimulation) and significantly higher potency in the cAMP assay. NOP partial agonists AT-004 and AT-200 also showed significantly higher potencies in the GIRK assay compared to that in the GTPγS assay (Table 2).

On the other hand, the compounds displayed lower efficacy at the MOR receptor in the GIRK assay, in rank order AT-200 > AT-312 > AT-004, compared to DAMGO, and the efficacy and potency obtained from the GIRK assay appeared to be somewhat consistent with those observed in the GTPγS assay. This is particularly true for the low-efficacy partial agonist AT-004, which showed low efficacy and poor potency at MOR in the GTPγS assay and showed no GIRK channel activation (Table 2).

Phosphorylation of NOP receptors induced by AT compounds. Using phosphosite-specific antibodies that we generated against residues in the NOP C-terminal tail, we previously showed

Molecular Pharmacology Fast Forward. Published on May 6, 2021 as DOI: 10.1124/molpharm.120.000076
This article has not been copyedited and formatted. The final version may differ from this version.

that N/OFQ-induced NOP receptor phosphorylation occurs in a time-dependent manner, where Ser346 phosphorylation occurred within 20 s, Ser351 phosphorylation occurred within 60 s and Thr362/Ser363 phosphorylation occurred after 3 min (Mann et al., 2019). Several known NOP agonists were also found to show varying profiles of phosphorylation after a 10-min exposure (Mann et al., 2019). Using the same phosphosite-specific antibodies, we next investigated the phosphorylation signatures of the AT NOP full agonists and partial agonists at a single timepoint, i.e. after exposure for 10 min, and at different concentrations. Figure 3 shows that NOP full agonist AT-403 induced strong phosphorylation at S346, S351 and T362/S363 (Figure 3A) at 10 μM concentration after a 10 min exposure, similar to N/OFQ. NOP full agonist AT-312, however, showed phosphorylation only at S346 and S351 at 1 and 10 μM concentrations, but no detectable phosphorylation at T362/S363 (Figure 3A) when measured at this single timepoint (i.e., after 10 min of incubation). Interestingly, NOP full agonist AT-390 showed no detectable phosphorylation at any of the three phosphosites at any concentration after 10 min of incubation (Figure 3A).

On the other hand, NOP partial agonists AT-004 and AT-200 showed no phosphorylation at 10 μM concentration at S351 and T362/S363 after 10 min of incubation (Figure 3A), but partial agonist AT-090 showed dose-dependent phosphorylation at all three sites, albeit more robust phosphorylation at S346 compared to the other two sites S351 and T362/S363 (Figure 3A).

Among the NOP full agonists examined here, only AT-403 was able to induce a multi-site phosphorylation profile similar to that of the endogenous agonist N/OFQ at all three sites probed within 10 min of incubation. In this regard, AT-403 appears to have a similar phosphorylation signature with other known NOP agonists that we have previously investigated (Ro64-6198, SCH221510, AT202 and MCOPPB, (Mann et al., 2019)) at similar time points. It is further

Molecular Pharmacology Fast Forward. Published on May 6, 2021 as DOI: 10.1124/molpharm.120.000076
This article has not been copyedited and formatted. The final version may differ from this version.

notable that, under these same conditions, NOP full agonist AT-390 induces no phosphorylation at the three phosphosites we probed, whereas full agonist AT-312 shows no receptor phosphorylation at T362/S363 but induces phosphorylation at the other two sites. These results indicate that at the 10-min time point, diverse NOP full agonists AT-403, AT-312 and AT-390 show differential but distinct receptor phosphorylation signatures.

Internalization of NOP receptors induced by AT compounds. NOP receptor internalization was visualized by fluorescence microscopy and quantified using a cell surface enzyme-linked immunosorbent assay (ELISA) (Figure 3B and 3C). In time-course experiments, we previously showed that NOP receptor internalization was first detectable after 5 min of agonist treatment and reached a maximum after 60 min (Mann et al., 2019). In initial experiments, internalization by N/OFQ, NOP full agonists AT-312, and partial agonists AT-004 and AT-200 was qualitatively characterized using fluorescence confocal microscopy (Figure 3B) after 60 min of agonist treatment. In subsequent experiments, internalization by N/OFQ, NOP full agonists AT-403 and AT-390, and partial agonist AT-090 after a 60-min treatment was characterized by a quantitative ELISA (Figure 3C). Figure 3B shows that N/OFQ induces robust internalization of the NOP receptor after 60 min of agonist exposure, further quantified by ELISA (in Figure 3C) as the percentage of internalized receptors in N/OFQ-treated cells. NOP full agonist AT-403, which showed a similar multi-site phosphorylation profile as N/OFQ after a 10-min exposure, showed a significantly lower level of receptor internalization compared to N/OFQ (Figure 3C) after the 60-min exposure. In Figure 3B, NOP full agonist AT-312, which also showed robust phosphorylation, appeared to show lower internalization compared to N/OFQ. On the other hand, NOP full agonist AT-390, which showed no phosphorylation (Figure 3A) after the 10-min

Molecular Pharmacology Fast Forward. Published on May 6, 2021 as DOI: 10.1124/molpharm.120.000076
This article has not been copyedited and formatted. The final version may differ from this version.

exposure, showed a level of receptor internalization not significantly different from that of N/OFQ itself (Figure 3C).

NOP partial agonist AT-090, which showed robust phosphorylation at S346 (Figure 3A), showed receptor internalization not significantly different than N/OFQ (Figure 3C), whereas partial agonists AT-004 and AT-200 showed little internalization of the NOP receptor (Figure 3B) after the 60-min exposure but also did not show phosphorylation at S351 or T362/S363.

Taken together, these results suggest that NOP phosphorylation at S346, S351 and T362/S363 may be sufficient, but not the only phosphorylated residues, to induce receptor internalization, and that phosphorylation at other as-yet unidentified residues in the intracellular domains of the NOP receptor is likely involved in receptor internalization induced by compounds such as AT390. The lower internalization observed with full agonist AT-403 compared to N/OFQ and AT-390, and the higher phosphorylation and internalization seen with partial agonist AT-090 compared to AT-004 and AT-200, further suggest that structurally diverse NOP ligands may induce differential receptor trafficking and receptor desensitization.

β-arrestin recruitment of AT compounds via NOP and MOR receptors. β-arrestin recruitment by selective NOP agonists is shown in Table 3 and in grpahs shown in Supplemental data Figure S4. The potency (EC_{50}) of the ligands and the % stimulation of β-arrestin recruitment normalized to that by N/OFQ are shown in Figure 4. NOP full agonist AT-403 showed significant β-arrestin recruitment with potency higher than that of N/OFQ, but with slightly lower efficacy (77% of N/OFQ recruitment). This lower efficacy for arrestin recruitment by AT-403 appears to be consistent with the lower % internalization observed with AT-403 compared to that of N/OFQ. NOP full agonist AT-390, which shows comparable NOP internalization (but not phosphorylation), shows significant β-arrestin recruitment with potency higher than N/OFQ itself

Molecular Pharmacology Fast Forward. Published on May 6, 2021 as DOI: 10.1124/molpharm.120.000076
This article has not been copyedited and formatted. The final version may differ from this version.

(Table 3). NOP full agonist AT-312 also shows nearly the same recruitment of β-arrestin with similar potency as N/OFQ. The rank order of β-arrestin recruitment by the synthetic NOP full agonists (AT-390>AT-312>AT-403) appears to be consistent with that for receptor internalization (AT-390>AT-403), but not phosphorylation, particularly for AT-312 and AT-390. Among NOP partial agonists, AT-090 shows higher stimulation of arrestin recruitment than N/OFQ itself (Table 3 and Figure S4). More importantly, even though AT-090 is a partial agonist of lower potency in the GTPγS assays, it shows the same potency as N/OFQ in the β-arrestin recruitment assay. Partial agonists AT-004 and AT-200 induced weak β-arrestin recruitment less than 50% of that induced by N/OFQ, and this appeared consistent with both their phosphorylation and internalization profiles.

At the MOR receptor, the selective NOP agonists AT-403, AT-390 and AT-312 had much lower potency for β-arrestin recruitment compared to the standard MOR agonist DAMGO (Table 3). Selective NOP partial agonist AT-004 showed undetectable recruitment of β-arrestin (Table 3). Modestly selective NOP partial agonist AT-200, which showed significant MOR partial agonist efficacy in the GTPγS assay and nearly full agonist efficacy in the GIRK assay (Table 2), had comparable potency for β-arrestin recruitment to MOR agonist DAMGO, albeit with lower efficacy (45% of DAMGO recruitment).

Overall, the efficacies of β-arrestin recruitment by the NOP agonists appeared to be associated with the levels of internalization observed for these NOP agonists. Figure 5 shows a graphical representation of the relative levels of β-arrestin recruitment and internalization for each NOP agonist, including N/OFQ, at the NOP receptor. NOP full agonist AT-390 and NOP partial agonist AT-090 both show comparatively higher β-arrestin recruitment and internalization than N/OFQ, whereas the other NOP full agonists AT-403 and AT-312, as well as NOP partial

Molecular Pharmacology Fast Forward. Published on May 6, 2021 as DOI: 10.1124/molpharm.120.000076
This article has not been copyedited and formatted. The final version may differ from this version.

agonists AT-004 and AT-200, showed lower β-arrestin recruitment and internalization. It is further notable that NOP full agonist AT-390, which shows higher β-arrestin recruitment and internalization than N/OFQ, shows no phosphorylation at any of the phosphosite residues we previously identified as being phosphorylated after N/OFQ binding (Mann et al., 2015). It is possible that residues other than the three phosphosites we probed with our available antibodies may be phosphorylated by NOP agonists such as AT-390 that lead to the robust β-arrestin recruitment and internalization observed with this nonpeptide NOP agonist.

Molecular Pharmacology Fast Forward. Published on May 6, 2021 as DOI: 10.1124/molpharm.120.000076
This article has not been copyedited and formatted. The final version may differ from this version.

DISCUSSION

In this study, we characterized the intrinsic activity of chemically diverse NOP agonists in various G protein-mediated functional assays (GTPγS binding, cAMP inhibition and GIRK activation) and characterized agonist-induced receptor trafficking by measuring ligand-induced NOP receptor phosphorylation of selected residues, arrestin recruitment and receptor internalization. Targeting the NOP receptor has been proposed by us and others as an approach to reduce the side effects of MOR agonists (Bird and Lambert, 2015; Gunther et al., 2018; Kiguchi et al., 2020a; Kiguchi et al., 2020b; Toll et al., 2009). Using an array of ligands, we showed that NOP agonists with varying functional selectivity towards the MOR receptor, i.e. NOP-MOR bifunctional agonists, achieve antinociception comparable to that seen with MOR agonists, but without the side effects of MOR such as opioid abuse liability, tolerance development and respiratory depression (Ding et al., 2018; Sukhtankar et al., 2013; Toll et al., 2009; Vang et al., 2015). Selective NOP receptor full agonists such as AT-312 and AT-202 reduce rewarding effects of several abused substances such as alcohol, cocaine as well as opioids (Toll et al., 2009; Zaveri et al., 2018a; Zaveri et al., 2018b). Other NOP full agonists such as AT-403 and AT-390 were found to attenuate the expression of levodopa-induced dyskinesia in animal models of Parkinson's disease (Arcuri et al., 2018). On the other hand, NOP receptor partial agonists such as AT-004 reduce parkinsonian motor symptoms in hemilesioned rats (Kamakolanu et al., 2020), whereas partial agonists like AT-090 were shown to have antidepressant-like properties in animal models (Asth et al., 2016).

NOP full agonists AT-403 and the well-characterized NOP agonist Ro 64-6198, have been found to disrupt motor and neurological function at higher doses (Arcuri et al., 2018; Higgins et al., 2001), an effect not observed with NOP partial agonists such as AT-004 or AT-090 (Asth et al., 2016; Kamakolanu et al., 2020). Since NOP receptor full agonists and partial agonists showed

Molecular Pharmacology Fast Forward. Published on May 6, 2021 as DOI: 10.1124/molpharm.120.000076
This article has not been copyedited and formatted. The final version may differ from this version.

varying levels of separation between therapeutically relevant effects and apparent motor suppressive activity, we undertook the detailed in vitro assessment of functional efficacies of these NOP agonists in assays of NOP receptor function and trafficking. It was hoped that these tools could elucidate the signaling profiles of NOP receptor agonists and provide information on differential effects of receptor regulation that may help explain the pharmacological effects of these NOP agonists.

Among the selective NOP agonists we examined, AT-312, AT-390 and AT-403 behaved as full agonists in the GTPγS assay, while AT-004, AT-090, and AT-200 showed lower efficacy and were partial agonists in this assay (Table 2). All these compounds showed even lower efficacy in the MOR GTPγS binding assay, confirming their selectivity for NOP agonist efficacy over MOR efficacy (Table 2).

Interestingly, however, we consistently found that ligands that appeared as partial agonists in the GTPγS assay showed significantly higher efficacy and potency as nearly full agonists in the cAMP and GIRK assays (Table 2). Comparison of intrinsic activities from the GTPγS, cAMP and GIRK assays revealed a systematically leftward shift of all dose-response events in cAMP and GIRK assays (Figure 2). The overestimation of agonist efficacy in the cAMP and GIRK assays was seen at both NOP and MOR receptors (Table 2). For example, while AT-004 showed only low efficacy for GTPγS binding at NOP, it behaved as a full agonist in the cAMP and GIRK assays (Table 2). Similarly, while AT-312 induced less than 30% stimulation in GTPγS binding at the MOR, it induced about 60% and >70% stimulation in the MOR cAMP and GIRK assays, respectively. Similar results were also observed with other AT compounds (Table 2). It is possible that higher efficacy seen in the cAMP and GIRK assays is due to signal amplification downstream in the signaling pathway. Intrinsic activity (% stimulation) measured in G protein

Molecular Pharmacology Fast Forward. Published on May 6, 2021 as DOI: 10.1124/molpharm.120.000076
This article has not been copyedited and formatted. The final version may differ from this version.

assays using heterologous transfected cell lines is also known to be affected by receptor reserve and signal amplification (Adham et al., 1993; Baker et al., 2000; Harrison and Traynor, 2003; McDonald et al., 2003; McDonald and Lambert, 2010). These factors may play a role in the different levels of agonist efficacy measured in these assays (Nickolls et al., 2011; Selley et al., 1997).

According to the classical model of agonist-induced GPCR activation, the agonist-bound receptor, complexed with G proteins, is phosphorylated by GRKs, and recruits β-arrestin, after which the receptor complex is targeted for internalization, leading to desensitization of the primary receptor signal. This study is the first to characterize several NOP agonists in these three main signaling nodes involved in NOP receptor trafficking after agonist binding, i.e. NOP receptor phosphorylation, β-arrestin recruitment and internalization was studied for each ligand. Our data presented interesting differences in the ability of various NOP agonists to induce these events. NOP full agonist AT-403 showed robust phosphorylation of all three examined phosphosites (S346, S351 and S362/S363) of NOP receptor after 10 min of incubation, comparable to the natural NOP full agonist N/OFQ (Figure 3A). NOP full agonist AT-312 also showed comparable phosphorylation at S346 and S351 but not at T362/S363 under similar exposure. NOP full agonist AT-390, on the other hand, showed no phosphorylation at any of these residues at any concentration under the same conditions. NOP partial agonists AT-004 and AT200 showed minimal phosphorylation of NOP receptor residues S351 and T362/S363 at 10 μM concentration (Figure 3A), whereas NOP partial agonist AT-090 showed a robust dose-dependent phosphorylation at all three sites after 10 min of incubation. The human NOP receptor contains several residues in its intracellular loops and C-terminal tail that can be potentially phosphorylated after receptor activation. Mann et al. reported that N/OFQ agonist-induced NOP

Molecular Pharmacology Fast Forward. Published on May 6, 2021 as DOI: 10.1124/molpharm.120.000076
This article has not been copyedited and formatted. The final version may differ from this version.

phosphorylation occurs primarily within the residues in the C-terminal tail (Mann et al., 2015). They generated phosphosite-specific antibodies to the C-terminal residues S346, S351 and T362/S363, and showed that N/OFQ and nonpeptide agonists showed a hierarchical and temporal phosphorylation of S346 followed by S351 and T363/S363 (Mann et al., 2015). In their study, the phosphorylation induced by N/OFQ and nonpeptide agonists appeared to correlate with the NOP internalization observed after treatment with these agonists. However, in the current study, the level of NOP internalization induced by the NOP agonists studied here did not appear to be consistent with the phosphorylation signatures induced by these agonists at the three phosphosites S346, S351 and T362/S363. Particularly, full agonist AT-390 showed no phosphorylation at any of these sites but still showed robust internalization compared to that by N/OFQ, which showed significant phosphorylation at all of these three residues. On the other hand, full agonist AT-403 showed similar phosphorylation to N/OFQ but lower internalization than N/OFQ (Figure 3C). Although ligand-induced receptor phosphorylation was probed after 10 min of incubation, whereas internalization was measured after 60 min exposure with NOP agonists, these results still suggest that residues other than S346/S351/T362/S363 are likely involved in ligand-induced NOP phosphorylation, leading to subsequent internalization particularly for NOP full agonist AT-390. Given that opioid receptor internalization leads to receptor desensitization, NOP full agonist AT-390 may induce more NOP desensitization compared to full agonist AT-403, which may lead to differences in the pharmacological responses between these two NOP full agonists. Indeed, we found that AT-403 and AT-390 showed different windows of separation between their anti-dyskinetic effects and disruption of locomotor activity (Arcuri et al., 2018).

Molecular Pharmacology Fast Forward. Published on May 6, 2021 as DOI: 10.1124/molpharm.120.000076
This article has not been copyedited and formatted. The final version may differ from this version.

The efficacy and potency of β-arrestin recruitment by these NOP full agonists appeared to be consistent with the internalization induced by these agonists (Figures 4 and 5). NOP full agonist AT-390 showed significantly higher arrestin recruitment with higher potency than the standard agonist N/OFQ. Interestingly, AT-390 also induces greater internalization than most other NOP full agonists we tested, including N/OFQ (Figure 3C). In contrast, the chemically distinct NOP full agonist AT-403 shows lower arrestin recruitment than N/OFQ (Table 3 and Supplemental Figure S4F) and also lower internalization than N/OFQ.

NOP receptor partial agonists AT-004 and AT-200 did not show significant arrestin recruitment, but partial agonist AT-090 showed a robust recruitment of β-arrestin, with potency and efficacy greater than N/OFQ itself (Table 3 and Supplemental Figure S4). AT-090 also showed significant receptor phosphorylation and robust internalization compared to N/OFQ and other full agonists. Thus, among NOP partial agonists characterized in this study, the internalization induced by AT-090 may suggest a greater propensity for receptor desensitization than NOP partial agonists AT-004 and AT-200.

In summary, the characterization of structurally diverse NOP full agonists and partial agonists presented here highlights the differential functional effects of chemically diverse NOP agonists on ligand-induced receptor signaling and trafficking. Furthermore, the results demonstrate that measurement of intrinsic activities of agonist ligands can vary with the type of functional assay used to measure intrinsic activity. These differences are particularly pronounced in the case of partial agonist ligands, which can show varying levels of agonist efficacies depending on the assay and system used. Therefore, characterizing GPCR agonist ligands as full agonists or partial agonists need to take into account several factors discussed above to determine intrinsic activity of agonist ligands. The differential effects on receptor trafficking, particularly of NOP full

Molecular Pharmacology Fast Forward. Published on May 6, 2021 as DOI: 10.1124/molpharm.120.000076
This article has not been copyedited and formatted. The final version may differ from this version.

agonist AT-390 and NOP partial agonist AT-090 compared to other NOP agonists may be important to understand the pharmacological profiles and actions of these NOP agonists.

Molecular Pharmacology Fast Forward. Published on May 6, 2021 as DOI: 10.1124/molpharm.120.000076
This article has not been copyedited and formatted. The final version may differ from this version.

Acknowledgments

The kind gift of the HTLA cell line stably expressing a tTA-dependent luciferase reporter and a β-arrestin2-TEV fusion gene, as well as corresponding plasmids for human NOP and MOR receptors, from Dr. Bryan Roth is gratefully acknowledged.

Molecular Pharmacology Fast Forward. Published on May 6, 2021 as DOI: 10.1124/molpharm.120.000076
This article has not been copyedited and formatted. The final version may differ from this version.

Authorship Contributions

Participated in research design: Lu, Mann, Schulz, and Zaveri

Conducted experiments: Lu, Polgar, Mann, and Dasgupta

Performed data analysis: Lu, Polgar, Mann, and Dasgupta

Wrote or contributed to the writing of the manuscript: Zaveri, Lu, Polgar, Schulz

Molecular Pharmacology Fast Forward. Published on May 6, 2021 as DOI: 10.1124/molpharm.120.000076
This article has not been copyedited and formatted. The final version may differ from this version.

REFERENCES

Adapa ID and Toll L (1997) Relationship between binding affinity and functional activity of nociceptin/orphanin FQ. *Neuropeptides* **31**(5): 403-408.

Adham N, Ellerbrock B, Hartig P, Weinshank RL and Branchek T (1993) Receptor reserve masks partial agonist activity of drugs in a cloned rat 5-hydroxytryptamine1B receptor expression system. *Mol Pharmacol* **43**(3): 427-433.

Allen JA, Yost JM, Setola V, Chen X, Sassano MF, Chen M, Peterson S, Yadav PN, Huang XP, Feng B, Jensen NH, Che X, Bai X, Frye SV, Wetsel WC, Caron MG, Javitch JA, Roth BL and Jin J (2011) Discovery of β-arrestin-biased dopamine D2 ligands for probing signal transduction pathways essential for antipsychotic efficacy. *Proc Natl Acad Sci U S A* **108**(45): 18488-18493.

Arcuri L, Novello S, Frassineti M, Mercatelli D, Pisano CA, Morella I, Fasano S, Journigan BV, Meyer ME, Polgar WE, Brambilla R, Zaveri NT and Morari M (2018) Anti-Parkinsonian and anti-dyskinetic profiles of two novel potent and selective nociceptin/orphanin FQ receptor agonists. *Br J Pharmacol* **175**(5): 782-796.

Asth L, Ruzza C, Malfacini D, Medeiros I, Guerrini R, Zaveri NT, Gavioli EC and Calo G (2016) Beta-arrestin 2 rather than G protein efficacy determines the anxiolytic-versus antidepressant-like effects of nociceptin/orphanin FQ receptor ligands. *Neuropharmacology* **105**: 434-442.

Baker SP, Scammells PJ and Belardinelli L (2000) Differential A(1)-adenosine receptor reserve for inhibition of cyclic AMP accumulation and G-protein activation in DDT(1) MF-2 cells. *Br J Pharmacol* **130**(5): 1156-1164.

Beedle AM, McRory JE, Poirot O, Doering CJ, Altier C, Barrere C, Hamid J, Nargeot J, Bourinet E and Zamponi GW (2004) Agonist-independent modulation of N-type calcium channels by ORL1 receptors. *Nature neuroscience* **7**(2): 118-125.

Bird MF and Lambert DG (2015) Simultaneous targeting of multiple opioid receptor types. *Current opinion in supportive and palliative care* **9**(2): 98-102.

Bunzow JR, Saez C, Mortrud M, Bouvier C, Williams JT, Low M and Grandy DK (1994) Molecular cloning and tissue distribution of a putative member of the rat opioid receptor gene family that is not a mu, delta or kappa opioid receptor type. *FEBS Lett* **347**(2-3): 284-288.

Molecular Pharmacology Fast Forward. Published on May 6, 2021 as DOI: 10.1124/molpharm.120.000076
This article has not been copyedited and formatted. The final version may differ from this version.

Camarda V, Fischetti C, Anzellotti N, Molinari P, Ambrosio C, Kostenis E, Regoli D, Trapella C, Guerrini R, Severo S and Calo G (2009) Pharmacological profile of NOP receptors coupled with calcium signaling via the chimeric protein G alpha qi5. *Naunyn Schmiedebergs Arch Pharmacol* **379**(6): 599-607.

Chang SD, Mascarella SW, Spangler S, Gurevich VV, Navarro HA, Carroll FI and Bruchas MR (2015) Quantitative Signaling and Structure-Activity Analyses Demonstrate Functional Selectivity at the Nociceptin/Orphanin FQ Opioid Receptor. *Molecular Pharmacology*.

Cheng Y and Prusoff WH (1973) Relationship between the inhibition constant (K1) and the concentration of inhibitor which causes 50 per cent inhibition (I50) of an enzymatic reaction. *Biochem Pharmacol* **22**(23): 3099-3108.

Connor M, Vaughan CW, Chieng B and Christie MJ (1996a) Nociceptin receptor coupling to a potassium conductance in rat locus coeruleus neurones in vitro. *Br J Pharmacol* **119**(8): 1614-1618.

Connor M, Yeo A and Henderson G (1996b) The effect of nociceptin on Ca2+ channel current and intracellular Ca2+ in the SH-SY5Y human neuroblastoma cell line. *Br J Pharmacol* **118**(2): 205-207.

Coward P, Chan SD, Wada HG, Humphries GM and Conklin BR (1999) Chimeric G proteins allow a high-throughput signaling assay of Gi-coupled receptors. *Analytical biochemistry* **270**(2): 242-248.

Ding H, Kiguchi N, Yasuda D, Daga PR, Polgar WE, Lu JJ, Czoty PW, Kishioka S, Zaveri NT and Ko MC (2018) A bifunctional nociceptin and mu opioid receptor agonist is analgesic without opioid side effects in nonhuman primates. *Sci Transl Med* **10**(456).

Donica CL, Awwad HO, Thakker DR and Standifer KM (2013) Cellular mechanisms of nociceptin/orphanin FQ (N/OFQ) peptide (NOP) receptor regulation and heterologous regulation by N/OFQ. *Mol Pharmacol* **83**(5): 907-918.

Ferrari F, Cerlesi MC, Malfacini D, Asth L, Gavioli EC, Journigan VB, Kamakolanu UG, Meyer MM, Yasuda D, Polgar WE, Rizzi A, Guerrini R, Ruzza C, Zaveri NT and Calo G (2016) In vitro functional characterization of novel nociceptin/orphanin FQ receptor agonists in recombinant and native preparations. *European Journal of Pharmacology* **793**: 1-13.

Ferrari F, Malfacini D, Journigan BV, Bird MF, Trapella C, Guerrini R, Lambert DG, Calo G and Zaveri NT (2017) In vitro pharmacological characterization of a novel unbiased NOP receptor-selective nonpeptide agonist AT-403. *Pharmacol Res Perspect* **5**(4): in press.

Fukuda K, Kato S, Mori K, Nishi M, Takeshima H, Iwabe N, Miyata T, Houtani T and Sugimoto T (1994) cDNA cloning and regional distribution of a novel member of the opioid receptor family. *FEBS Lett* **343**(1): 42-46.

Gillis A, Sreenivasan V and Christie MJ (2020) Intrinsic efficacy of opioid ligands and its importance for apparent bias, operational analysis and therapeutic window. *Mol Pharmacol*.

Günther T, Culler M and Schulz S (2016) Research Resource: Real-Time Analysis of Somatostatin and Dopamine Receptor Signaling in Pituitary Cells Using a Fluorescence-Based Membrane Potential Assay. *Mol Endocrinol* **30**(4): 479-490.

Gunther T, Dasgupta P, Mann A, Miess E, Kliewer A, Fritzwanker S, Steinborn R and Schulz S (2018) Targeting multiple opioid receptors - improved analgesics with reduced side effects? *Br J Pharmacol* **175**(14): 2857-2868.

Harrison C and Traynor JR (2003) The [35S]GTPgammaS binding assay: approaches and applications in pharmacology. *Life Sci* **74**(4): 489-508.

Hawes BE, Graziano MP and Lambert DG (2000) Cellular actions of nociceptin: transduction mechanisms. *Peptides* **21**(7): 961-967.

Higgins GA, Grottick AJ, Ballard TM, Richards JG, Messer J, Takeshima H, Pauly-Evers M, Jenck F, Adam G and Wichmann J (2001) Influence of the selective ORL1 receptor agonist, Ro64-6198, on rodent neurological function. *Neuropharmacology* **41**(1): 97-107.

Hill SJ, Williams C and May LT (2010) Insights into GPCR pharmacology from the measurement of changes in intracellular cyclic AMP; advantages and pitfalls of differing methodologies. *Br J Pharmacol* **161**(6): 1266-1275.

Ikeda K, Kobayashi K, Kobayashi T, Ichikawa T, Kumanishi T, Kishida H, Yano R and Manabe T (1997) Functional coupling of the nociceptin/orphanin FQ receptor with the G-protein-activated K+ (GIRK) channel. *Brain Res Mol Brain Res* **45**(1): 117-126.

Kamakolanu UG, Meyer ME, Yasuda D, Polgar WE, Marti M, Mercatelli D, Pisano CA, Brugnoli A, Morari M and Zaveri NT (2020) Discovery and Structure-Activity

Relationships of Nociceptin Receptor Partial Agonists That Afford Symptom Ablation in Parkinson's Disease Models. *J Med Chem* **63**(5): 2688-2704.

Kelly E (2013) Efficacy and ligand bias at the μ-opioid receptor. *Br J Pharmacol* **169**(7): 1430-1446.

Khroyan TV, Polgar WE, Orduna J, Montenegro J, Jiang F, Zaveri NT and Toll L (2011) Differential Effects of Nociceptin/Orphanin FQ (NOP) Receptor Agonists in Acute versus Chronic Pain: Studies with Bifunctional NOP/mu Receptor Agonists in the Sciatic Nerve Ligation Chronic Pain Model in Mice. *Journal of Pharmacology and Experimental Therapeutics* **339**(2): 687-693.

Kiguchi N, Ding H, Kishioka S and Ko MC (2020a) Nociceptin/orphanin FQ peptide receptor-related ligands as novel analgesics. *Curr Top Med Chem*.

Kiguchi N, Ding H and Ko MC (2020b) Therapeutic potentials of NOP and MOP receptor coactivation for the treatment of pain and opioid abuse. *J Neurosci Res*.

Knapman A, Abogadie F, McIntrye P and Connor M (2014) A real-time, fluorescence-based assay for measuring μ-opioid receptor modulation of adenylyl cyclase activity in Chinese hamster ovary cells. *J Biomol Screen* **19**(2): 223-231.

Lachowicz JE, Shen Y, Monsma FJ, Jr. and Sibley DR (1995) Molecular cloning of a novel G protein-coupled receptor related to the opiate receptor family. *J Neurochem* **64**(1): 34-40.

Malfacini D, Ambrosio C, Gro MC, Sbraccia M, Trapella C, Guerrini R, Bonora M, Pinton P, Costa T and Calo G (2015) Pharmacological Profile of Nociceptin/Orphanin FQ Receptors Interacting with G-Proteins and beta-Arrestins 2. *PLoS One* **10**(8): e0132865.

Mandyam CD, Thakker DR, Christensen JL and Standifer KM (2002) Orphanin FQ/nociceptin-mediated desensitization of opioid receptor-like 1 receptor and mu opioid receptors involves protein kinase C: a molecular mechanism for heterologous cross-talk. *J Pharmacol Exp Ther* **302**(2): 502-509.

Mandyam CD, Thakker DR and Standifer KM (2003) Mu-opioid-induced desensitization of opioid receptor-like 1 and mu-opioid receptors: differential intracellular signaling determines receptor sensitivity. *J Pharmacol Exp Ther* **306**(3): 965-972.

Mann A, Illing S, Miess E and Schulz S (2015) Different mechanisms of homologous and heterologous mu-opioid receptor phosphorylation. *Br J Pharmacol* **172**(2): 311-316.

Molecular Pharmacology Fast Forward. Published on May 6, 2021 as DOI: 10.1124/molpharm.120.000076
This article has not been copyedited and formatted. The final version may differ from this version.

Mann A, Mouledous L, Froment C, O'Neill PR, Dasgupta P, Gunther T, Brunori G, Kieffer BL, Toll L, Bruchas MR, Zaveri NT and Schulz S (2019) Agonist-selective NOP receptor phosphorylation correlates in vitro and in vivo and reveals differential post-activation signaling by chemically diverse agonists. *Sci Signal* **12**(574).

McDonald J, Barnes TA, Okawa H, Williams J, Calo G, Rowbotham DJ and Lambert DG (2003) Partial agonist behaviour depends upon the level of nociceptin/orphanin FQ receptor expression: studies using the ecdysone-inducible mammalian expression system. *Br J Pharmacol* **140**(1): 61-70.

McDonald J and Lambert DG (2010) Binding of GTPgamma[35S] is regulated by GDP and receptor activation. Studies with the nociceptin/orphanin FQ receptor. *Br J Pharmacol* **159**(6): 1286-1293.

Meunier JC, Mollereau C, Toll L, Suaudeau C, Moisand C, Alvinerie P, Butour JL, Guillemot JC, Ferrara P, Monsarrat B, Mazarguil H, Vassart G, Parmentier M and Costentiná J (1995) Isolation and structure of the endogenous agonist of opioid receptor-like ORL1 receptor. *Nature* **377**(6549): 532-535.

Mollereau C, Parmentier M, Mailleux P, Butour JL, Moisand C, Chalon P, Caput D, Vassart G and Meunier JC (1994) ORL1, a novel member of the opioid receptor family. Cloning, functional expression and localization. *FEBS Lett* **341**(1): 33-38.

Nickolls SA, Waterfield A, Williams RE and Kinloch RA (2011) Understanding the effect of different assay formats on agonist parameters: a study using the μ-opioid receptor. *J Biomol Screen* **16**(7): 706-716.

Parsons MP and Hirasawa M (2011) GIRK channel-mediated inhibition of melanin-concentrating hormone neurons by nociceptin/orphanin FQ. *Journal of neurophysiology* **105**(3): 1179-1184.

Reinscheid RK, Nothacker HP, Bourson A, Ardati A, Henningsen RA, Bunzow JR, Grandy DK, Langen H, Monsma FJ, Jr. and Civelli O (1995) Orphanin FQ: a neuropeptide that activates an opioidlike G protein-coupled receptor. *Science* **270**(5237): 792-794.

Selley DE, Liu Q and Childers SR (1998) Signal transduction correlates of mu opioid agonist intrinsic efficacy: receptor-stimulated [35S]GTP gamma S binding in mMOR-CHO cells and rat thalamus. *J Pharmacol Exp Ther* **285**(2): 496-505.

Molecular Pharmacology Fast Forward. Published on May 6, 2021 as DOI: 10.1124/molpharm.120.000076
This article has not been copyedited and formatted. The final version may differ from this version.

Selley DE, Sim LJ, Xiao R, Liu Q and Childers SR (1997) mu-Opioid receptor-stimulated guanosine-5`-O-(gamma-thio)-triphosphate binding in rat thalamus and cultured cell lines: signal transduction mechanisms underlying agonist efficacy. *Mol Pharmacol* **51**: 87.

Sim LJ, Xiao R and Childers SR (1996) Identification of opioid receptor-like (ORL1) peptide-stimulated [35S]GTP gamma S binding in rat brain. *Neuroreport* **7**(3): 729-733.

Sukhtankar DD, Zaveri NT, Husbands SM and Ko MC (2013) Effects of spinally administered bifunctional nociceptin/orphanin FQ peptide receptor/mu-opioid receptor ligands in mouse models of neuropathic and inflammatory pain. *J Pharmacol Exp Ther* **346**(1): 11-22.

Thakker DR and Standifer KM (2002) Induction of G protein-coupled receptor kinases 2 and 3 contributes to the cross-talk between mu and ORL1 receptors following prolonged agonist exposure. *Neuropharmacology* **43**(6): 979-990.

Toll L, Bruchas MR, Calo G, Cox BM and Zaveri NT (2016) Nociceptin/Orphanin FQ Receptor Structure, Signaling, Ligands, Functions, and Interactions with Opioid Systems. *Pharmacol Rev* **68**(2): 419-457.

Toll L, Khroyan TV, Polgar WE, Jiang F, Olsen C and Zaveri NT (2009) Comparison of the antinociceptive and antirewarding profiles of novel bifunctional nociceptin receptor/mu-opioid receptor ligands: implications for therapeutic applications. *J Pharmacol Exp Ther* **331**(3): 954-964.

Traynor JR and Nahorski SR (1995) Modulation by mu-opioid agonists of guanosine-5`-O-(3-[35S]thio)triphosphate binding to membranes from human neuroblastoma SH-SY5Y cells. *Mol Pharmacol* **47**: 848.

Vang D, Paul JA, Nguyen J, Tran H, Vincent L, Yasuda D, Zaveri NT and Gupta K (2015) Small-molecule nociceptin receptor agonist ameliorates mast cell activation and pain in sickle mice. *Haematologica* **100**(12): 1517-1525.

Vaughan CW and Christie MJ (1996) Increase by the ORL1 receptor (opioid receptor-like1) ligand, nociceptin, of inwardly rectifying K conductance in dorsal raphe nucleus neurones. *Br J Pharmacol* **117**(8): 1609-1611.

Williams JT, Ingram SL, Henderson G, Chavkin C, von Zastrow M, Schulz S, Koch T, Evans CJ and Christie MJ (2013) Regulation of μ-opioid receptors: desensitization, phosphorylation, internalization, and tolerance. *Pharmacol Rev* **65**(1): 223-254.

Zaveri N, Polgar WE, Olsen CM, Kelson AB, Grundt P, Lewis JW and Toll L (2001) Characterization of opiates, neuroleptics, and synthetic analogs at ORL1 and opioid receptors. *Eur J Pharmacol* **428**(1): 29-36.

Zaveri NT, Jiang F, Olsen Cris M, Deschamps Jeffrey R, Parrish D, Polgar W and Toll L (2004) A novel series of piperidin-4-yl-1,3-dihydroindol-2-ones as agonist and antagonist ligands at the nociceptin receptor. *Journal of Medicinal Chemistry* **47**: 2973--2976.

Zaveri NT, Marquez PV, Meyer ME, Hamid A and Lutfy K (2018a) The Nociceptin Receptor (NOP) Agonist AT-312 Blocks Acquisition of Morphine- and Cocaine-Induced Conditioned Place Preference in Mice. *Front Psychiatry* **9**: 638.

Zaveri NT, Marquez PV, Meyer ME, Polgar WE, Hamid A and Lutfy K (2018b) A novel and selective nociceptin receptor (NOP) agonist (1-(1-((cis)-4-isopropylcyclohexyl) piperidin-4-yl)-1H-indol-2-yl)methanol (AT-312) decreases acquisition of ethanol-induced conditioned place preference in mice. *Alcoholism Clinical and Experimental Research* **42**: 461-471.

Zhang NR, Planer W, Siuda ER, Zhao HC, Stickler L, Chang SD, Baird MA, Cao YQ and Bruchas MR (2012) Serine 363 is required for nociceptin/orphanin FQ opioid receptor (NOPR) desensitization, internalization, and arrestin signaling. *J Biol Chem* **287**(50): 42019-42030.

Molecular Pharmacology Fast Forward. Published on May 6, 2021 as DOI: 10.1124/molpharm.120.000076
This article has not been copyedited and formatted. The final version may differ from this version.

Footnotes

This work was supported by the National Institutes of Health's National Institute on Drug Abuse [Grants R01DA027811 and R44DA042465 to NTZ].

Conflict of Interest Statement

All authors declare no conflict of interest.

Reprint requests should be sent to:

Dr. Nurulain T. Zaveri

Astraea Therapeutics, LLC.

320 Logue Avenue, Suite 142,

Mountain View, CA 94043, USA.

Tel: 650-254-0786

Email: nurulain@astraeatherapeutics.com

Molecular Pharmacology Fast Forward. Published on May 6, 2021 as DOI: 10.1124/molpharm.120.000076
This article has not been copyedited and formatted. The final version may differ from this version.

Figure Legends

Figure 1. Chemical Structures of NOP agonists investigated.

Figure 2. Maximal stimulation of G-protein signaling of human NOP receptor by NOP agonists, measured in GTPγS, cAMP and GIRK assays, and normalized to N/OFQ (100%). Each value represents the average value and standard deviations obtained from three experiments done on different days, with triplicates in each experiment.

Figure 3. Phosphorylation and internalization induced by AT compounds at human NOP receptor. A: HEK293 cells expressing human NOP receptors were treated with 10 μM of N/OFQ, AT-004, AT-200, AT-403, or vehicle (−), or 1 nM to 10 μM of AT-090, AT-312, and AT-390, at 37 ^{o}C for 10 min, and cell lysates were immunoblotted with antibodies to pSer346, pSer351 or pThr362/Ser363. Blots were stripped and reprobed for human NOP receptor to ensure equal loading. All blots were representative of 3-5 experiments. B: HEK293 cells stably expressing HA-tagged human NOP receptors were pre-incubated with HA antibody and then stimulated with 10 μM of N/OFQ, AT-004, AT-200, AT-312, or solvent vehicle at 22 ^{o}C for 60 min. Cells were then fixed, permeabilized, stained immunofluorescently, and examined subsequently using confocal microscopy. All images were representative of three independent experiments. C: HEK293 cells stably expressing human NOP receptors were pre-incubated with antibody to HA-tag and treated with 10 μM of N/OFQ, AT-390, AT-090, or AT-403 at 37 ^{o}C for 60 min. Then, the cells were fixed and labeled with a peroxidase-conjugated secondary antibody. Receptor internalization was measured by ELISA and quantified as the percentage of internalized receptors in the cells treated with agonists. Data represents mean ± standard deviations from 12 independent experiments performed in quadruplicate. The *P* values were comparative to N/OFQ

Molecular Pharmacology Fast Forward. Published on May 6, 2021 as DOI: 10.1124/molpharm.120.000076
This article has not been copyedited and formatted. The final version may differ from this version.

and were obtained using two sample Student's t tests assuming unequal variances. *: $p < 0.05$ vs. N/OFQ.

Figure 4. Stimulation of β-arrestin recruitment at human NOP receptor induced by AT-004, AT-090, AT-200, AT-312, AT-390, and AT-403, normalized to N/OFQ (100%). On Day 1, HTLA cells were plated at 10×10^6 cells in 150 mm cell culture dishes. On Day 2, the cells were transfected with NOP receptor plasmids using the Fugene 6 HD transfection reagent. On Day 3, transfected cells were harvested by trypsinization and then transferred into white flat-bottom 96-well tissue culture plates. On Day 4, the cells were treated with corresponding AT compounds or N/OFQ control overnight at 37 ^{o}C for at least 18 h. On Day 5, the luciferase reading in each well was detected by using a Bright Glo Luciferase Reporter Assay on a plate reader. % β-arrestin recruitment was normalized to that of N/OFQ (at 1 μM). Each experiment was repeated at least 3 times, with each drug concentration in quintuplicate wells to obtain the average value ± standard deviation. The potency (EC_{50} nM) of each NOP agonist for β-arrestin recruitment is labeled in the graph for each agonist.

Figure 5. Graphical side-by-side representation of the levels of NOP receptor internalization and β-arrestin recruitment by NOP agonists.

Molecular Pharmacology Fast Forward. Published on May 6, 2021 as DOI: 10.1124/molpharm.120.000076
This article has not been copyedited and formatted. The final version may differ from this version.

Table 1. Receptor binding affinities of NOP ligands at the human NOP and human MOR receptors expressed in CHO cells*.

Compound	**hNOP K_i nM** (number of independent experiments)	**hMOR K_i nM** (number of independent experiments)	**Selectivity (fold over hMOR binding) (hMOR K_i/hNOP K_i)**
N/OFQ	0.12 ± 0.01**	-	-
DAMGO	-	0.59 ± 0.03**	-
AT-004	9.8 ± 0.9 (4)	375.5 ± 36.5 (4)	38-fold
AT-090	5.6 ± 1.7 (3)	95.4 ± 3.5 (3)	17-fold
AT-200	4.1 ± 0.1 (4)	107.1 ± 8.9 (7)	26-fold
AT-312	0.3 ± 0.1 (6)	6.0 ± 1.0 (6)	20-fold
AT-390	0.9 ± 0.3 (5)	53.1 ± 16.5 (5)	59-fold
AT-403	1.1 ± 0.1 (4)	97.9 ± 15.0 (7)	91-fold

*Binding affinities were determined using radioligand displacement assays as described in *Materials and Methods*. Equilibrium dissociation constants (K_i) were derived from IC_{50} values using the Cheng−Prusoff equation. Each K_i value represents the arithmetic mean ± standard deviation calculated from corresponding number of independent experiments, with each experiment performed in triplicate. **The number of N/OFQ and DAMGO binding experiments was not labeled since each experiment of AT compounds was accompanied with N/OFQ or DAMGO as the standard.

Molecular Pharmacology Fast Forward. Published on May 6, 2021 as DOI: 10.1124/molpharm.120.000076
This article has not been copyedited and formatted. The final version may differ from this version.

Table 2. Functional assays of G-protein signaling

hNOP						
Compound	**GTPγS**		**cAMP**		**GIRK**	
	EC_{50} (nM)	Emax (%Stim)	EC_{50} (nM)	Emax (%Stim)	EC_{50} (nM)	Emax (%Stim)
N/OFQ	3.6 ± 0.7	100	2.2 ± 1.8	100	1.2 ± 0.2	100
DAMGO	-----	-----	-----	-----	N.A.	< 5.0
hNOP Full Agonists						
AT312	29.9 ± 1.4	102.3 ± 0.8	14.9 ± 7.6	98.0 ± 12.9	1.8 ± 0.2	105.8 ± 3.4
AT390	15.2 ± 0.4	110.1 ± 11.4	12.6 ± 1.3	98.3 ± 5.8	ND	ND
AT403	6.3 ± 1.4	104.6 ± 1.2	3.7 ± 4.5	105.9 ± 4.1	ND	ND
hNOP Partial Agonists						
AT-004	266.6 ± 73.7	39.7 ± 4.5	224.8 ± 123.4	84.8 ± 19.9	11.2 ± 2.7	97.9 ± 4.5
AT-090	50.1±6.4	21.0±6.5	4.5±2.1	104.6±11.6	ND	ND
AT-200	27.2 ± 0.8	55.5 ± 0.7	23.6 ± 11.3	89.3 ± 6.6	3.2 ± 0.6	99.0 ± 3.4
hMOR						
Compound	**GTPγS**		**cAMP**		**GIRK**	
	EC_{50} (nM)	Emax (%Stim)	EC_{50} (nM)	Emax (%Stim)	EC_{50} (nM)	Emax (%Stim)
N/OFQ	-----	-----	-----	-----	N.A.	< 5.0
DAMGO	32.6 ± 4.1	100	9.1 ±4.9	100	1.0 ± 0.2	100
AT-004	231.7 ± 10.3	16.3 ± 7.6	N.A.	13.3 ± 0.3	N.A.	< 5.0
AT-090	N.A.	6.0 ± 2.8	354.9 ± 75.9	84.7 ± 7.8	ND	ND
AT-200	68.0 ± 9.3	43.5 ± 14.7	59.2 ± 31.1	87.4 ± 2.7	75.4 ± 42.0	59.3 ± 4.8
AT-312	81.5 ± 16.0	24.6 ± 2.4	378.4 ± 28.4	60.4 ± 12.0	149.2 ± 32.6	76.2 ± 2.8
AT-390	143.8 ± 0.6	54.3 ± 9.4	100.3 ± 26.0	88.4 ± 1.0	ND	ND
AT-403	206.4 ± 78.9	33.5 ± 14.6	160.5 ± 56.4	81.2 ± 5.7	ND	ND

Molecular Pharmacology Fast Forward. Published on May 6, 2021 as DOI: 10.1124/molpharm.120.000076
This article has not been copyedited and formatted. The final version may differ from this version.

Note: Emax (%Stim): Percentage of stimulation compared to that of the control NOF/Q or DAMGO, as described in Methods. “N.A.” indicates not detectable; “ND” indicates not done. All results are expressed as mean ± standard deviation calculated from at least 3 independent experiments.

Molecular Pharmacology Fast Forward. Published on May 6, 2021 as DOI: 10.1124/molpharm.120.000076
This article has not been copyedited and formatted. The final version may differ from this version.

Table 3. Functional assays of phosphorylation, internalization and β-arrestin recruitment

Compound	hNOP				hMOR	
	Phosphorylation Intensity	Internalization (%)	β-arrestin recruitment		β-arrestin recruitment	
			EC_{50} (nM)	% Recruitment	EC_{50} (nM)	% Recruitment
N/OFQ	+	100	14.3±9.0	100±2.7	----	----
DAMGO	-	---	----	----	46.5±22.7	100±1.3
AT-004	-	50	N.A.	26.7±8.4	N.A.	6.6±0.1
AT-090	low	74	17.8 ±	146.3±37.4	175.0±80.3	84.4±7.2
AT-200	low	25	241.0±56.	41.3±4.7	29.6±27.1	45.1±2.9
AT-312	-	50	6.8±3.5	97.3±10.7	175.0±28.2	84.5±9.8
AT-390	-	122	6.3±4.5	247.4±64.8	165.0±2.1	78.9±4.1
AT-403	+	65	4.3±3.2	77.8±12.1	475.0±196.	92.1±7.3

Note: %Recruitment: Percentage of β-arrestin recruitment compared to that induced by the control NOF/Q or DAMGO, as described in Methods.

"-" indicates no phosphorylation, "+" indicates strong phosphorylation, "low" indicates a low level of phosphorylation between 10%-30%, "N.A." indicates not available. The EC_{50} and %Recruitment values of β-arrestin recruitment are expressed as mean ± standard deviation calculated from at least 3 independent experiments

Molecular Pharmacology Fast Forward. Published on May 6, 2021 as DOI: 10.1124/molpharm.120.000076
This article has not been copyedited and formatted. The final version may differ from this version.

Figure 1.

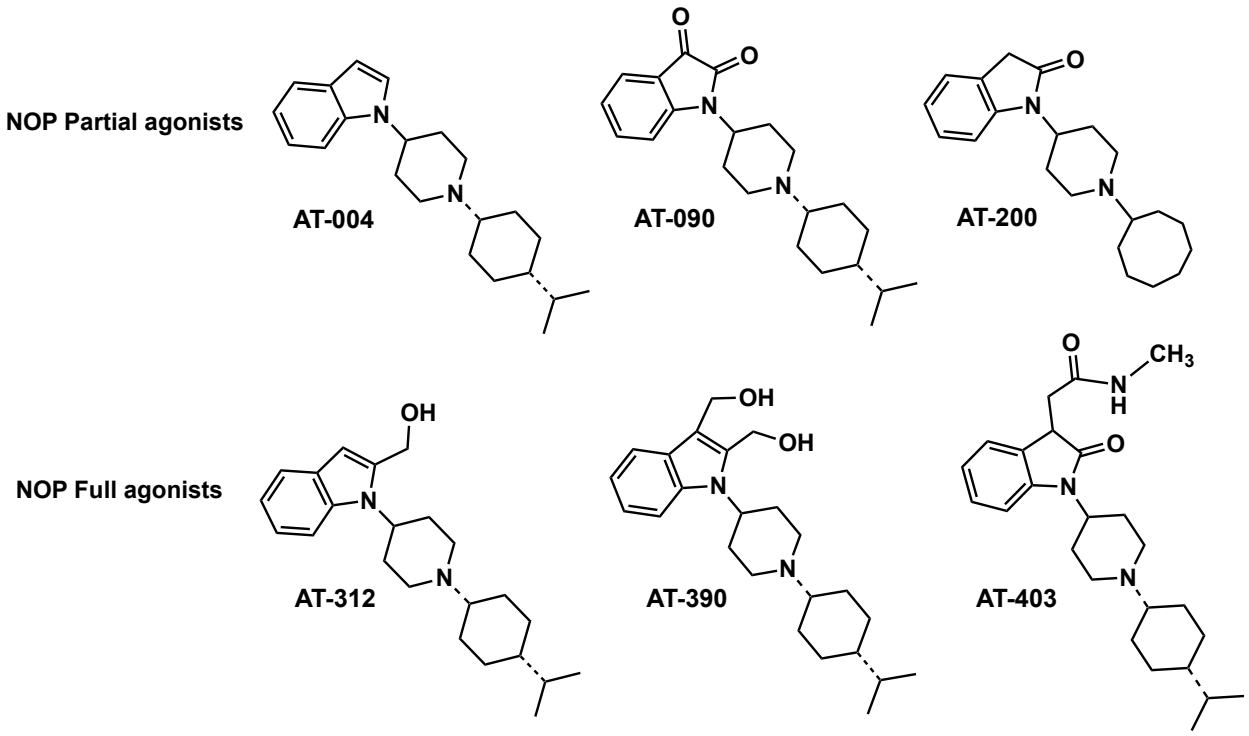

Molecular Pharmacology Fast Forward. Published on May 6, 2021 as DOI: 10.1124/molpharm.120.000076
This article has not been copyedited and formatted. The final version may differ from this version.

Figure 2.

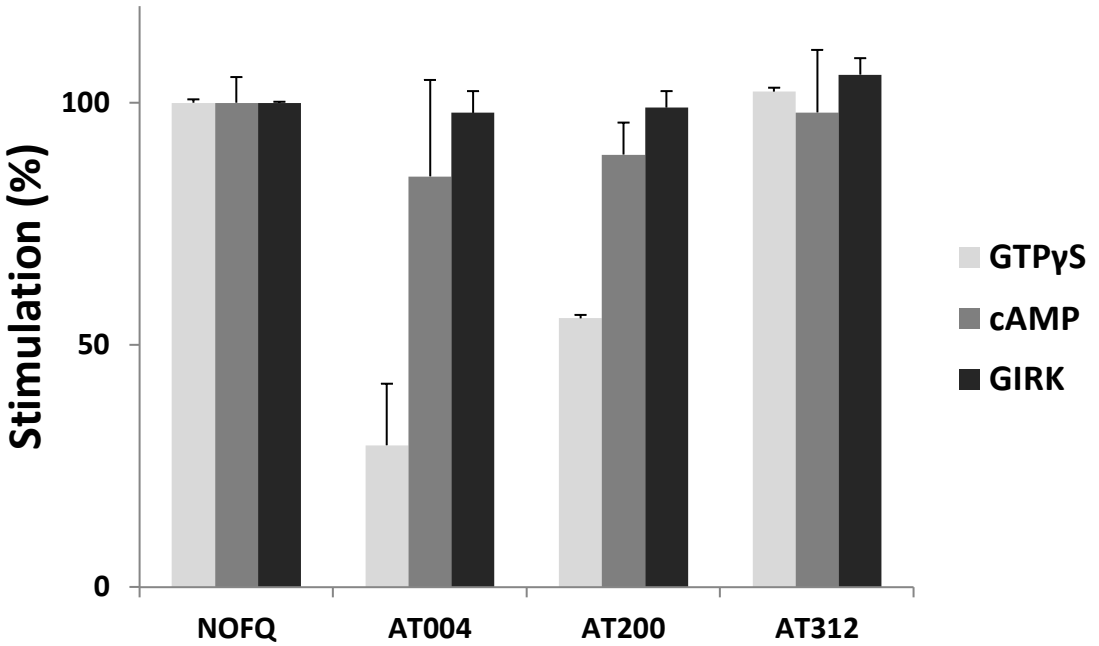

Molecular Pharmacology Fast Forward. Published on May 6, 2021 as DOI: 10.1124/molpharm.120.000076
This article has not been copyedited and formatted. The final version may differ from this version.

Figure 3.

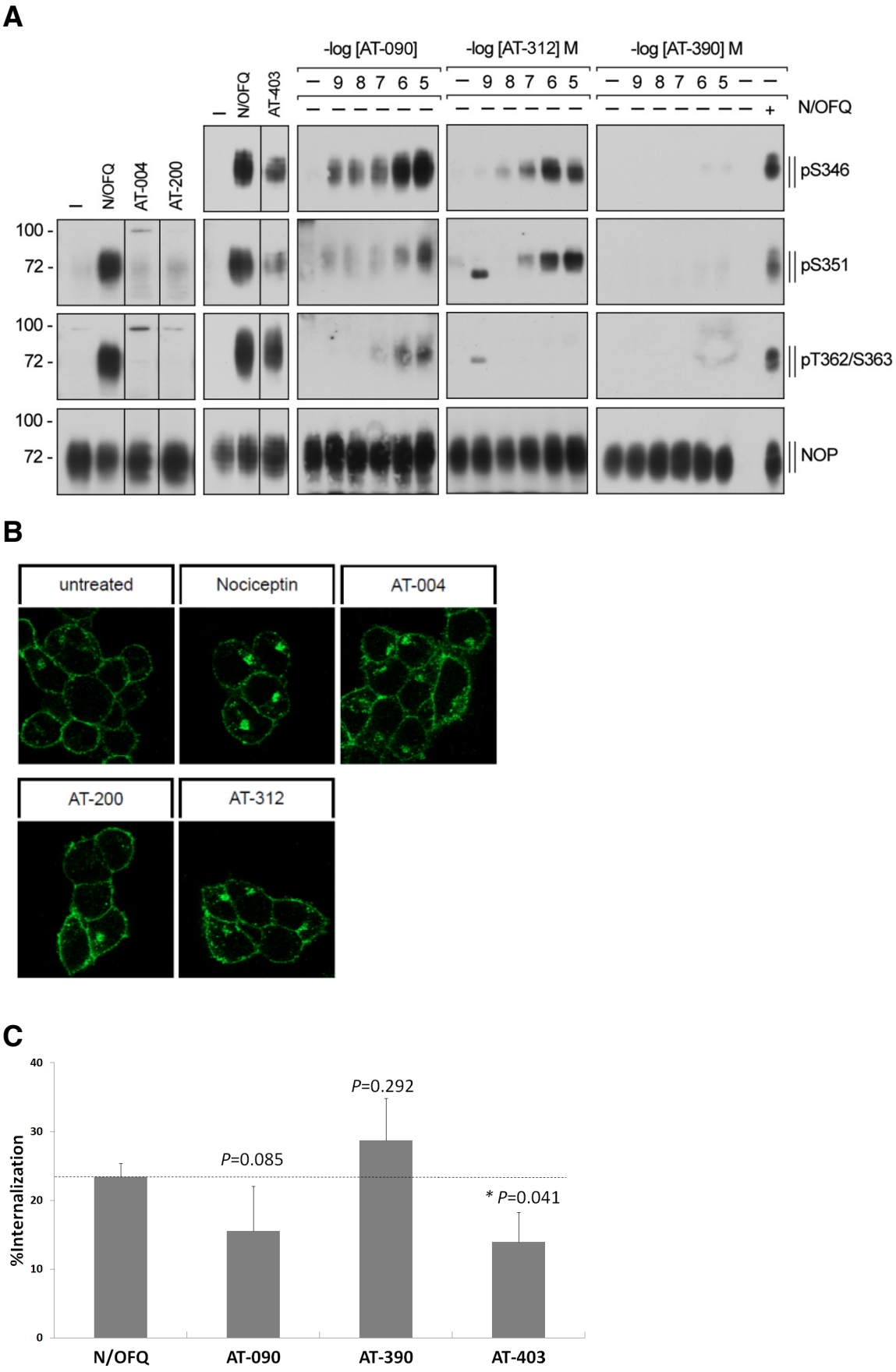

Figure 4.

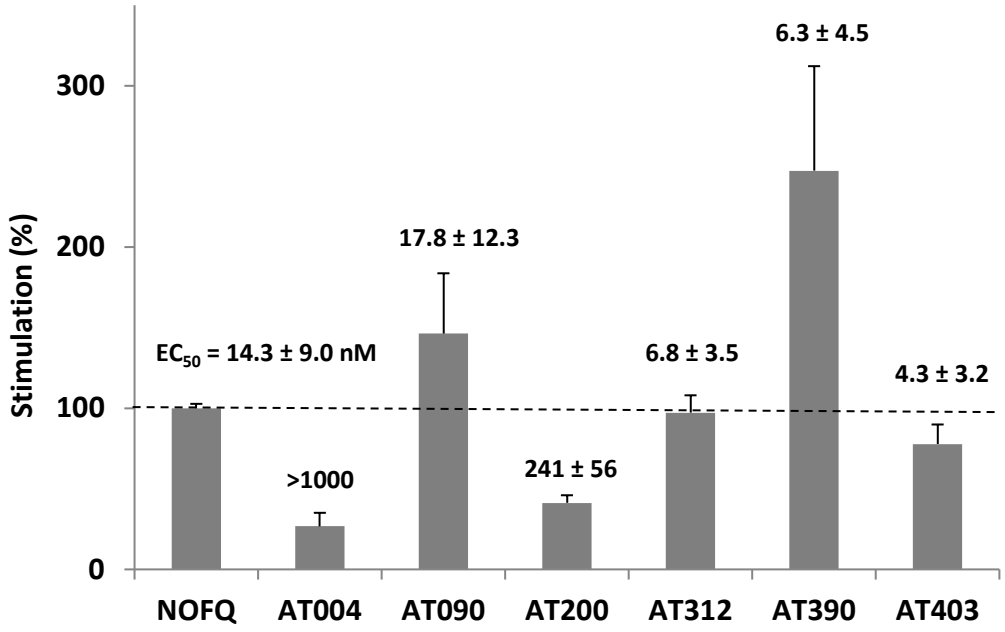
Stimulation (%)
300
200
100
0
EC50 = 14.3 ± 9.0 nM
>1000
17.8 ± 12.3
241 ± 56
6.8 ± 3.5
6.3 ± 4.5
4.3 ± 3.2
NOFQ
AT004
AT090
AT200
AT312
AT390
AT403

Figure 5.

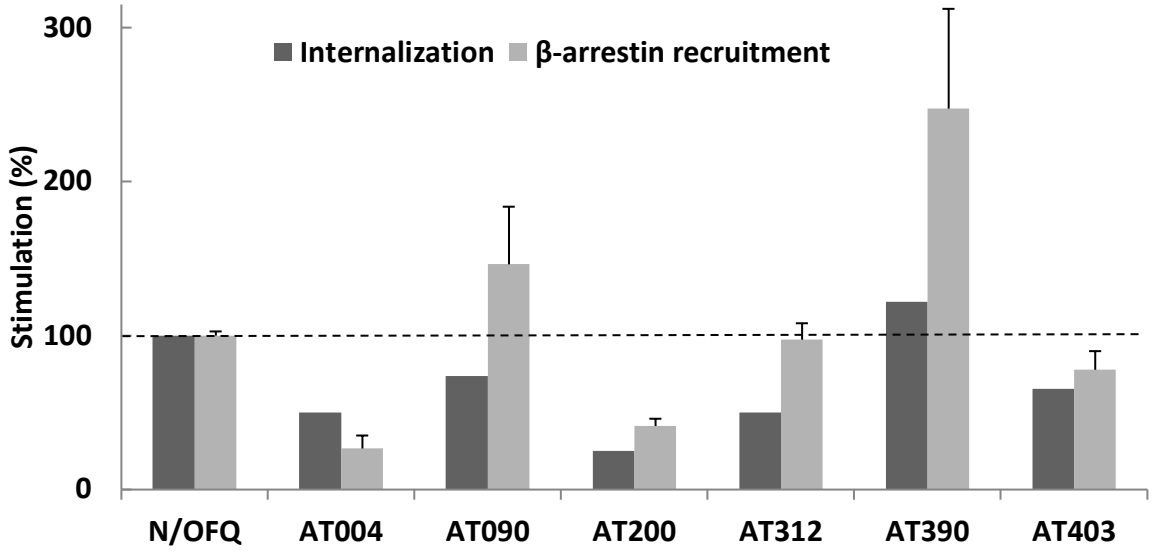
Internalization
β-arrestin recruitment
Stimulation (%)
300
200
100
0
N/OFQ
AT004
AT090
AT200
AT312
AT390
AT403